UCSF
UC San Francisco Previously Published Works

Title
Ion transport and regulation in a synaptic vesicle glutamate transporter

Permalink
https://escholarship.org/uc/item/35z0z0cn

Journal
Science, 368(6493)

ISSN
0036-8075

Authors
Li, Fei
Eriksen, Jacob
Finer-Moore, Janet
et al.

Publication Date
2020-05-22

DOI
10.1126/science.aba9202

Peer reviewed

eScholarship.org Powered by the California Digital Library
University of California

Author Manuscript

Author Manuscript

Author Manuscript

Author Manuscript

HHS Public Access

Author manuscript

Science. Author manuscript; available in PMC 2020 July 29.

Published in final edited form as:

Science. 2020 May 22; 368(6493): 893–897. doi:10.1126/science.aba9202.

Ion transport and regulation in a synaptic vesicle glutamate transporter

Fei Li[1,2], **Jacob Eriksen**[2], **Janet Finer-Moore**[1], **Roger Chang**[2,3,*], **Phuong Nguyen**[1], **Alisa Bowen**[1], **Alexander Myasnikov**[1,†], **Zanlin Yu**[1], **David Bulkley**[1], **Yifan Cheng**[1,4], **Robert H. Edwards**[2,‡], **Robert M. Stroud**[1,‡]

[1]Department of Biochemistry and Biophysics, University of California San Francisco (UCSF) School of Medicine, San Francisco, CA, USA.

[2]Departments of Neurology and Physiology, UCSF School of Medicine, San Francisco, CA, USA.

[3]Graduate Program in Biomedical Sciences, UCSF, San Francisco, CA, USA.

[4]Howard Hughes Medical Institute, UCSF, San Francisco, CA, USA.

Abstract

Synaptic vesicles accumulate neurotransmitters, enabling the quantal release by exocytosis that underlies synaptic transmission. Specific neurotransmitter transporters are responsible for this activity and therefore are essential for brain function. The vesicular glutamate transporters (VGLUTs) concentrate the principal excitatory neurotransmitter glutamate into synaptic vesicles, driven by membrane potential. However, the mechanism by which they do so remains poorly understood owing to a lack of structural information. We report the cryo–electron microscopy structure of rat VGLUT2 at 3.8-angstrom resolution and propose structure-based mechanisms for substrate recognition and allosteric activation by low pH and chloride. A potential permeation pathway for chloride intersects with the glutamate binding site. These results demonstrate how the activity of VGLUTs can be coordinated with large shifts in proton and chloride concentrations during the synaptic vesicle cycle to ensure normal synaptic transmission.

The storage of neurotransmitters inside synaptic vesicles enables their release by regulated exocytosis, conferring the vesicular (or quantal) release that mediates synaptic transmission (1). Synaptic vesicles take up classical neurotransmitters [monoamines, acetylcholine, γ-aminobutyric acid (GABA), and glutamate] from the cytosol, mediated by specific vesicular neurotransmitter transporters (VNTs) (2). A proton electrochemical gradient ($\Delta\mu_{H+}$ = ΔpH +

‡ Corresponding author. stroud@msg.ucsf.edu (R.M.S.); robert.edwards@ucsf.edu (R.H.E.).
*Present address: Department of Neurology, University of Washington, School of Medicine, Seattle, WA, USA.
†Present address: Cryo-Electron Microscopy and Tomography Center, St. Jude Children's Research Hospital, Memphis, TN, USA.

Author contributions: F.L., R.M.S., and R.H.E. conceived the project. F.L., P.N., and A.B. expressed the protein. F.L. purified the protein; prepared all samples for EM; acquired cryo-EM data with the help of A.M., Z.Y., and D.B.; and determined the structure of VGLUT2. Y.C. advised on cryo-EM experiments. J.E. and R.C. performed the functional experiments. F.L., J.F.-M., and R.M.S. analyzed the structure. F.L., J.F.-M., R.H.E., and R.M.S. wrote the manuscript.

Competing interests: The authors declare no competing interests.

Data and materials availability: The atomic coordinates of rat VGLUT2 have been deposited in the Protein Data Bank with the accession code 6V4D. The corresponding map has been deposited in the Electron Microscopy Data Bank with the accession code EMD-21040.

Author Manuscript Author Manuscript Author Manuscript Author Manuscript

$\Delta\psi$) generated by the vacuolar adenosine triphosphatase (V-ATPase) across the synaptic vesicle membrane drives this uptake by all VNTs, but the VNTs vary in their dependence on the chemical gradient (ΔpH) and the membrane potential ($\Delta\psi$) component of $\Delta\mu_{H+}$ (2). Vesicular glutamate transporters (VGLUTs) package the major excitatory neurotransmitter glutamate, driven predominantly by $\Delta\psi$ (3, 4). A $\Delta\psi$ of −80 mV alone suffices to concentrate glutamate ~20-fold to the observed luminal concentration of >100 mM, which enables the activation of postsynaptic receptors upon vesicle fusion and the release of concentrated neurotransmitter into the synaptic cleft. However, the mechanism by which these transporters function remains poorly understood in the absence of structural information.

As synaptic vesicles cycle at the nerve terminal, the rapidly changing ionic conditions also impose a series of challenges for the regulation of VGLUTs (2). The positive outside resting potential of the cell membrane resembles the synaptic vesicle membrane potential. Once vesicles have fused with the plasma membrane, VGLUTs become resident in the plasma membrane and could cause nonquantal release of glutamate because of the positive outside membrane potential. Upon reinternalization from the plasma membrane, vesicles trap extracellular solution with ~120 mM Cl^- and neutral pH, conditions that are unfavorable for glutamate filling. The high concentration of luminal glutamate required for synaptic transmission necessitates a corresponding displacement of the luminal Cl^-. To cope with these challenges, the VGLUTs exhibit complex interactions with H^+ and Cl^- (4–13). Additionally, excessive release of glutamate can produce excitotoxicity (14), and misregulation of the VGLUTs has been implicated in psychiatric and neurodegenerative diseases (15, 16). However, the mechanisms that underlie the regulation of VGLUTs have remained unidentified.

Mammals express three closely related VGLUT isoforms (75% sequence identity; fig. S1). The two major isoforms VGLUT1 and VGLUT2 exhibit complementary expression in, respectively, the cortex and diencephalon (17), and the loss of either impairs survival (18, 19). Because rat VGLUT2 is only 65 kDa, we determined its structure at 3.8-Å resolution by cryo-electron microscopy (cryo-EM) facilitated by an antigen-binding fragment (Fab) (Fig. 1A and figs. S2 and S3). Densities corresponding to lipids or detergents lie parallel to the VGLUT2 helices (fig. S4). The structure of VGLUT2 was determined de novo (fig. S5 and table S1) and adopts a canonical major facilitator superfamily (MFS) fold (Fig. 1, B and C). Consistent with an MFS transporter that uses the alternating access mechanism, most transmembrane (TM) helices are distorted or kinked by proline and/or glycine (20). Reflecting its function in transporting a negatively charged substrate, the central cavity of VGLUT2 is positively charged (Fig. 1D).

Although VGLUT2 was captured in a luminal (outward) open apo state, comparison with other family members illuminates the basis for substrate specificity. The nine members of the SLC17 family in humans transport diverse organic anions, including glutamate (VGLUT1, VGLUT2, and VGLUT3), sialic acid (sialin), ATP [vesicular nucleotide transporter (VNUT)], and urates [sodium-phosphate transporters (NPTs)] (21) (Fig. 2A). Among their substrates, glutamate is the only one with two carboxyl groups. In VGLUT2, positively charged R88 orients toward the central binding site (Fig. 2B) and is conserved,

Author Manuscript Author Manuscript Author Manuscript Author Manuscript

which is consistent with a common role in anion recognition by the SLC17 family. The equivalent residue (R47) in the bacterial homolog D-galactonate transporter (DgoT) makes a salt bridge with the carboxyl group of its substrate D-galactonate (22) (Fig. 2C). R322 faces R88 from the opposite side of the binding site. Consistent with recognition of the second carboxyl in glutamate, R322 is conserved among the VGLUTs but not in other SLC17 family members. When glutamate is manually placed into the central cavity to mimic D-galactonate in DgoT, R88 and R322 can coordinate the two carboxyl groups (Fig. 2B). We tested the role of R88 and R322 in synaptic transmission by measuring miniature excitatory postsynaptic currents (mEPSCs) caused by the release of single synaptic vesicles from VGLUT1 and VGLUT2 double knockout hippocampal neurons rescued by wild-type (WT) and mutant VGLUT2. In contrast to the wild type, the R88A mutant drastically impairs synaptic transmission, whereas R322A eliminates release (Fig. 2D and fig. S6A). Both mutations also eliminate glutamate currents recorded from endosomes expressing VGLUT2 (13). We speculate that low levels of residual activity may enable R88 (but not R322) to fill synaptic vesicles undergoing spontaneous release, which have a long time to fill. The two arginines are well matched to the distance between substrate carboxyl groups, and, accordingly, aspartate is not transported by the VGLUTs (3, 5). In addition to R88 and R322, the substrate binding site is surrounded by aromatic and polar residues. Consistent with recognition of the carboxyl group common to SLC17 substrates, Y135 is also conserved (Fig. 2B).

Both R88 and R322 interact with clusters of charged and polar residues buried within the N- and C-domains through coulombic interactions (fig. S7, A to D). These networks connect substrate binding by R88 and R322 with titratable regulatory sites within the transmembrane domains. The R88 cluster (Fig. 3, A to C) in the N-domain includes residues conserved throughout the SLC17 family. In contrast, the R322 cluster (Fig. 3, A and D) in the C-domain includes a histidine (H487)–glutamate (E396) pair 3.0 Å apart and C321, all of which are specifically conserved only in the VoGLUTs (fig. S1), which suggests a possible role in binding the second carboxyl group of glutamate.

The allosteric regulation of VGLUTs by H^+ provides a mechanism to prevent glutamate efflux to the synaptic cleft when VGLUTs translocate from the synaptic vesicle (pH ~5.6) to the presynaptic plasma membrane (pH ~7.4) during exocytosis. In hippocampal neurons, external high pH blocks the nonvesicular efflux of glutamate by VGLUT expressed on the plasma membrane (11, 23), which limits the potential for tonic excitation and excitotoxicity. Protons act allosterically to gate the VGLUT-associated Cl^- conductance (11) and, because of the similar regulation, we infer a similar allosteric mechanism for the activation of glutamate transport. In VGLUT2, E191 lies in the center of the N-domain within the buried, charged R88 cluster (Fig. 3, A to C). E191 is highly conserved in TM4 of the VGLUTs, and mutations of E191 reduce transport activity (24). The equivalent residue in DgoT (E133) is essential for H^+ symport (22) and is conserved in the H^+ symporter sialin (fig. S1). Consistent with a role in H^+ recognition, a glutamate is not present at this position in ATP or urate transporters, which are not H^+ driven (fig. S1). These factors and the environment of E191 support the idea of a role for E191 as a luminal H^+ sensor; protonation of this residue may liberate the adjacent R88 to interact with the substrate. In the case of DgoT and sialin, substrate transport is stoichiometrically coupled to the flux of H^+. In contrast, VGLUT2 has

Author Manuscript Author Manuscript Author Manuscript Author Manuscript

lost the obligatory coupling of H^+ to substrate, thereby minimizing the potential leakage of glutamate from the H^+-rich synaptic vesicle (25) and allowing the uptake of glutamate against the synaptic vesicle H^+ gradient. Thus, E191 appears to have undergone a transition in role from H^+ coupling in DgoT and sialin to allosteric activation by H^+ in the VGLUTs. However, because E191 is buried, H128—partially exposed to the lumen and specific to VGLUTs—could act as the initial H^+ binding site from the lumen. It is also connected to E191 by a polar, water-filled tunnel with a minimum diameter of 1.8 Å (fig. S8A).

Located at the center of the R88 cluster, R184 in TM4 interacts with the backbone of I127 and H128 in TM2 as well as the backbone of R88 in TM1 (Fig. 3, B and C). R184 is proposed to confer allosteric activation by Cl^- because the neutralization of this residue eliminates the requirement for luminal Cl^- (13). R184 is conserved in all SLC17 proteins that generally depend on Cl^- (26). The positive charge on R184 interacts electrostatically with E191 and the entire R88 cluster (fig. S7, E and F). Hence, neutralization of the charge on R184 by Cl^- binding will have a large effect on the structure of the R88 cluster and will favor protonation of E191 (i.e., raise the pK_a, where K_a is the acid association constant). Similarly, protonation of E191 may favor Cl^- binding to R184.

The volume close to both R184 and H128—which are 5.2 Å apart—is large enough to accommodate a hydrated Cl^- ion (with a diameter of 3.6 Å). Tunnels with minimum diameters of 2.2 to 2.8 Å allow ready access for Cl^- to this site (fig. S8B). Chloride ions are most often coordinated by arginine, histidine, and serine (27), and hydrophobic surfaces are often seen surrounding tunnels, for example in ClC channels, or in excitatory amino acid transporters (EAATs). Thus, proximity of R184 to H128 may render the Cl^- binding subject to regulation by luminal acidic pH (11) and more than ~30 mM luminal Cl^- (13), so both are required to activate the VGLUTs. The current structure of VGLUT2 at pH 7.4, in an inhibited state, suggests that neutral pH may deprotonate H128 and so might inhibit Cl^- binding in the vicinity of H128 and R184. We do not see a Cl^- ion in the binding site under these conditions with 150 mM NaCl. However, Cl^- has a large negative form factor for electron scattering at low resolution (infinity to 16 Å) that may diminish any density. High-pass filtering to higher resolution did not reveal any additional density. Therefore, it is also reasonable that a weakly bound, hydrated chloride could be at this site in the structure. Consistent with their roles, mutations of R184 or H128 in VGLUT2 substantially reduce activity (24). The proximity of the H^+ and Cl^- binding sites explains the interdependence of pH and Cl^- that has been observed in the literature (4, 6, 11, 28).

It has been proposed that a VGLUT-associated Cl^- conductance enables the removal of Cl^- trapped during endocytosis to make room for glutamate (8, 11–13). The Cl^- conductance competes with glutamate transport (7), and mutation of the glutamate-binding R322 (as in R322A) abolishes the Cl^- conductance (11, 13) (fig. S6C). Together, these observations imply that the Cl^- channel intersects with the glutamate binding site. The R88A mutation also abolishes the Cl^- conductance of VGLUT2 (fig. S6B). The most commensurate channel, defined by a solvent-accessible surface of sufficient internal diameter to support a Cl^- ion, runs through the central cavity between substrate-binding R88 and R322 to a cytoplasmic gate formed by two histidine residues (H199 in the N-domain and H434 in the C-domain) that oppose each other (Fig. 4, A to C). This two-His gate is specific to the

Author Manuscript Author Manuscript Author Manuscript Author Manuscript

VGLUTs and sialin and is not present in other SLC17 family proteins. The two histidine residues are not hydrogen-bonded to each other; rather both H199 and H434 side chains donate hydrogen bonds to the backbone carbonyl of N431 (Fig. 4C). The hydrogen bond from H199 would contribute to the stabilization of the observed conformation, which is closed to the cytoplasmic side. Consistent with the role of H199 in forming and breaking this hydrogen bond that is critical for conformation change, a natural mutation of the equivalent residue in sialin (H183R) abolishes sialic acid transport and causes infantile sialic acid storage disease (29, 30). The channel narrows to 2.4-Å diameter at the two-His gate, which requires small rearrangements to allow the conductance of Cl^- with a diameter of 3.6 Å. This parallels the Cl^- channel in TMEM16A, which has a similar diameter and characteristics and also narrows to 2.5 Å (31). With the two-His gate closed, the channel splits into two exits to the cytoplasmic side (Fig. 4A, purple). Both exit channels are too narrow to permit Cl^- permeation without rearrangement of the gate upon Cl^- entry. A third discontinuous channel (Fig. 4A, pink) leads from the two-His gate to the cytosol and is lined by residues conserved in the VGLUTs. This channel may also allow Cl^- to exit throughout the transport cycle.

On the basis of the structure presented in this study, we propose a transport mechanism and regulatory scheme for the VGLUTs (Fig. 4D). The electrochemical environment in the synaptic vesicles (low pH and >30 mM Cl^-) activates VGLUTs, whereas neutral pH at the plasma membrane inhibits VGLUTs, thus minimizing nonvesicular efflux. Under activating conditions, glutamate is transported through alternating access, bound by positive charges on R88 and R322 that stabilize the two negative charges of glutamate. This ensures that there is no insidious cotransport of H^+ on the substrate, against the proton gradient, into the vesicle, with its associated energy cost. This is in contrast to closely related H^+-symporters DgoT and sialin. Upon substrate delivery by VGLUTs, the positive charge inside the vesicle favors the retention of the negatively charged substrate. Cl^- may contribute to neutralizing excess positive charge on VGLUT and promote recycling in the absence of substrate, thereby playing a role in the reorientation from the luminal open structure. Thus, the overall transport cycle delivers substrate to a lower energy state in the lumen and allows the concentration of glutamate to >100 mM. In the plasma membrane after exocytosis, neutral pH drives VGLUTs to an inactive, outward-open conformation where both the H^+ and Cl^- binding sites are empty (current structure). Transport would only resume after endocytosis, synaptic vesicle regeneration, and acidification, thereby integrating allosteric activation by H^+ at E191 mediated through H128, and by Cl^- at R184, with the synaptic vesicle cycle. A Cl^- channel intersecting with the glutamate binding site allows movement of Cl^- to balance electrostatic potential within— and osmotic forces across—the synaptic vesicle and to potentially determine an upper limit for vesicular glutamate concentration.

Supplementary Material

Refer to Web version on PubMed Central for supplementary material.

ACKNOWLEDGMENTS

We thank M. Braunfeld and M. Harrington at the UCSF cryo-EM facility for their support in data acquisition and computation. We are also grateful for discussions with N. Poweleit, K. Verba, J.-P. Armache, M. Sun, A. Brilot, E.

Author Manuscript Author Manuscript Author Manuscript Author Manuscript

Green, and D. Asarnow regarding the cryo-EM. We also thank D. Cawley at the Vaccine and Gene Therapy Institute (Oregon Health and Science University) for generating the mAb and for advice on working with the antibodies; C. Craik, M. Bohn, and K. Basu for advice and help in characterizing and working with antibodies; and S. Schenck and R. Dutzler for sharing nanobodies against *r*VGLUT1 used during preliminary characterization and structural determinations efforts.

Funding: This work is supported by R01NS089713 to R.M.S. and R.H.E. and R37MH50712 to R.H.E. F.L. is supported by postdoctoral fellowships from the American Heart Association (17POST33660928) and the National Institute of Mental Health (K99MH119591). The UCSF Electron Microscopy (EM) facility is supported by NIH grants S10OD020054 and S10OD021741. Y.C. is a Howard Hughes Medical Institute Investigator.

REFERENCES AND NOTES

1. Katz B, Science 173, 123–126 (1971). [PubMed: 4325812]
2. Edwards RH, Neuron 55, 835–858 (2007). [PubMed: 17880890]
3. Maycox PR, Deckwerth T, Hell JW, Jahn R, J. Biol. Chem 263, 15423–15428 (1988). [PubMed: 2902091]
4. Tabb JS, Kish PE, Van Dyke R, Ueda T, J. Biol. Chem 267, 15412–15418 (1992). [PubMed: 1353494]
5. Naito S, Ueda T, J. Neurochem 44, 99–109 (1985). [PubMed: 2856886]
6. Wolosker H, de Souza DO, de Meis L, J. Biol. Chem 271, 11726–11731 (1996). [PubMed: 8662610]
7. Bellocchio EE, Reimer RJ, Fremeau RT Jr., Edwards RH, Science 289, 957–960 (2000). [PubMed: 10938000]
8. Schenck S, Wojcik SM, Brose N, Takamori S, Nat. Neurosci 12, 156–162 (2009). [PubMed: 19169251]
9. Goh GY et al., Nat. Neurosci 14, 1285–1292 (2011). [PubMed: 21874016]
10. Preobraschenski J, Zander JF, Suzuki T, Ahnert-Hilger G, Jahn R, Neuron 84, 1287–1301 (2014). [PubMed: 25433636]
11. Eriksen J et al., Neuron 90, 768–780 (2016). [PubMed: 27133463]
12. Martineau M, Guzman RE, Fahlke C, Klingauf J, Nat. Commun 8, 2279 (2017). [PubMed: 29273736]
13. Chang R, Eriksen J, Edwards RH, eLife 7, e34896 (2018). [PubMed: 30040066]
14. Lau A, Tymianski M, Pflugers Arch. 460, 525–542 (2010). [PubMed: 20229265]
15. Kashani A, Betancur C, Giros B, Hirsch E, El Mestikawy S, Neurobiol. Aging 28, 568–578 (2007). [PubMed: 16563567]
16. Oni-Orisan A, Kristiansen LV, Haroutunian V, Meador-Woodruff JH, McCullumsmith RE, Biol. Psychiatry 63, 766–775 (2008) [PubMed: 18155679]
17. Fremeau RT Jr. et al., Neuron 31, 247–260 (2001). [PubMed: 11502256]
18. Wojcik SM et al., Proc. Natl. Acad. Sci. U.S.A 101, 7158–7163 (2004). [PubMed: 15103023]
19. Wallén-Mackenzie A et al., J. Neurosci 26, 12294–12307 (2006). [PubMed: 17122055]
20. Yan N, Annu. Rev. Biophys 44, 257–283 (2015). [PubMed: 26098515]
21. Reimer RJ, Mol. Aspects Med 34, 350–359 (2013). [PubMed: 23506876]
22. Leano JB et al., PLOS Biol. 17, e3000260 (2019). [PubMed: 31083648]
23. Mackenzie B, Illing AC, Morris ME, Varoqui H, Erickson JD, Neurochem. Res. 33, 238–247 (2008). [PubMed: 18080752]
24. Juge N, Yoshida Y, Yatsushiro S, Omote H, Moriyama Y, J. Biol. Chem 281, 39499–39506 (2006). [PubMed: 17046815]
25. Takami C, Eguchi K, Hori T, Takahashi T, J. Physiol 595, 1263–1271 (2017). [PubMed: 27801501]
26. Hiasa M, Togawa N, Moriyama Y, Curr. Pharm. Des 20, 2745–2749 (2014). [PubMed: 23886392]
27. Carugo O, BMC Struct Biol. 14, 19 (2014). [PubMed: 25928393]
28. Hartinger J, Jahn R, J. Biol. Chem 268, 23122–23127 (1993). [PubMed: 8226829]
29. Morin P, Sagné C, Gasnier B, EMBO J. 23, 4560–4570 (2004). [PubMed: 15510212]

Author Manuscript Author Manuscript Author Manuscript Author Manuscript

30. Wreden CC, Wlizla M, Reimer RJ, J. Biol. Chem 280, 1408–1416 (2005). [PubMed: 15516337]
31. Paulino C, Kalienkova V, Lam AKM, Neldner Y, Dutzler R, Nature 552, 421–425 (2017). [PubMed: 29236691]

Author Manuscript Author Manuscript Author Manuscript Author Manuscript

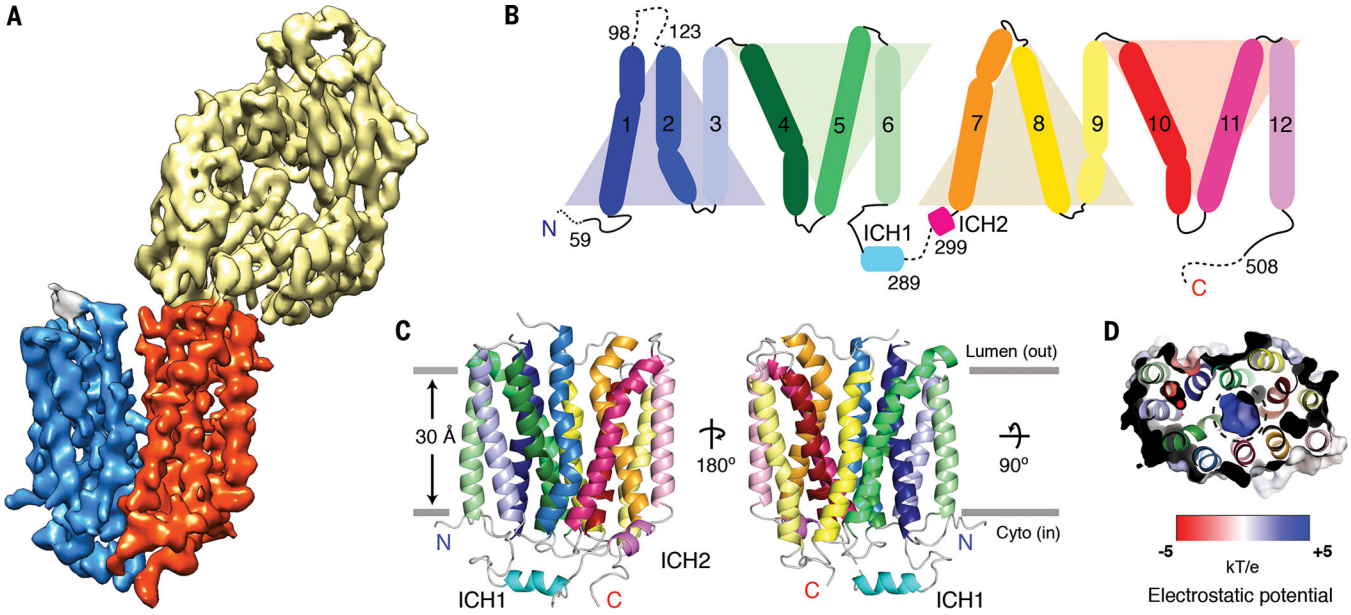

Fig. 1. Structure of VGLUT2.

(**A**) Cryo-EM map of the VGLUT2-Fab complex. The two domains are colored blue (N-domain) and red (C-domain), and the Fab is colored yellow. (**B**) Schematic representation of the structural arrangement of VGLUT2. Three-helix bundles are related to each other by a twofold pseudosymmetry, and each bundle is colored using shades of the same color group. (**C**) Structure of VGLUT2. Helices are colored according to the representation in (B), with connecting strands shown in gray. The VGLUT2 structure includes residues 59 to 508 except for the disordered loop 1 between TM1 and TM2 (residues 98 to 123) and 10 residues between ICH1 and ICH2 (residues 288 to 299). (**D**) Electrostatic surface of VGLUT2 shown at the plane parallel to the membrane through the central substrate binding site of the protein. The central cavity is indicated by a black dashed circle.

Author Manuscript Author Manuscript Author Manuscript Author Manuscript

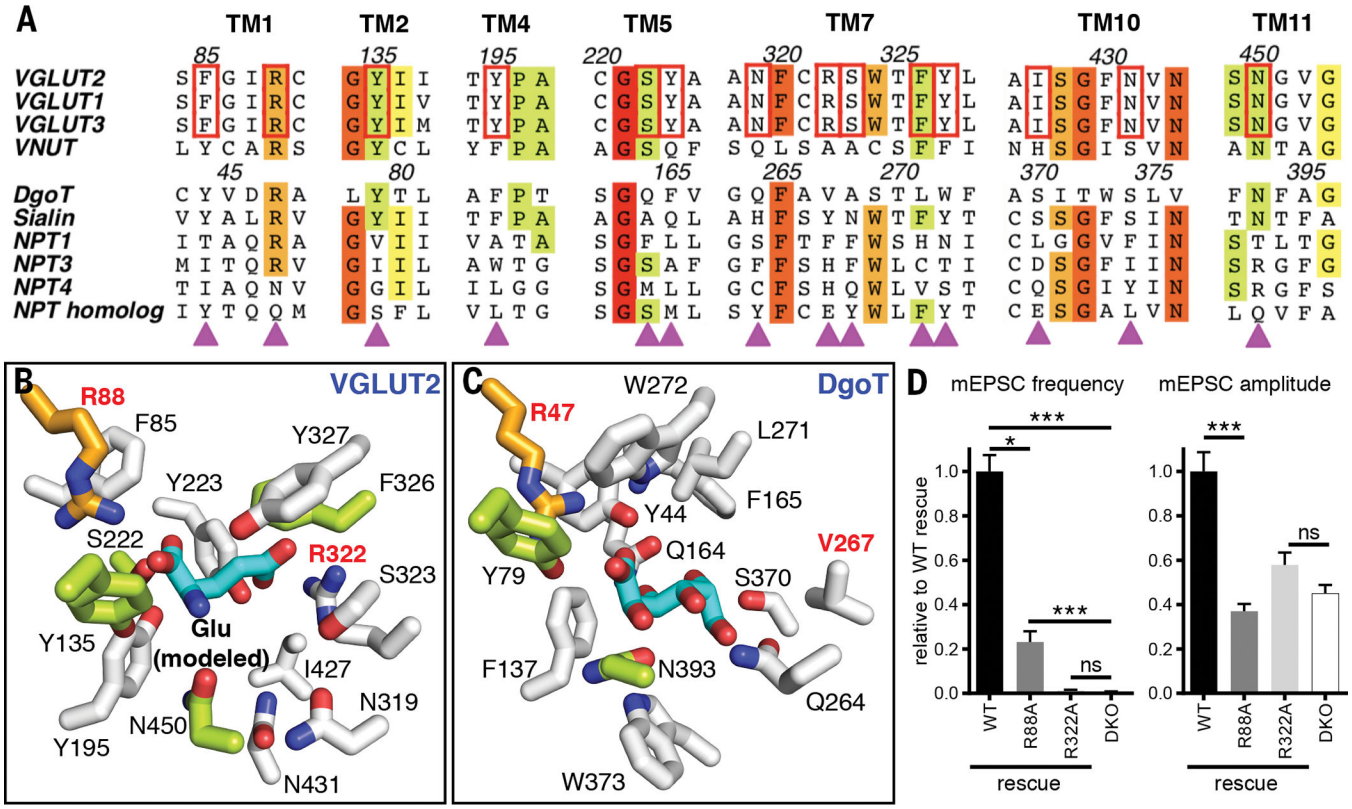

Fig. 2. R88 and R322 are critical for glutamate transport.

(**A**) Alignment of human SLC17 family proteins, presented alongside the *Escherichia coli* homolog DgoT, with binding site residues indicated by magenta triangles. Residues are colored according to sequence conservation in descending order of red, orange, yellow, green, and no color. Putative substrate binding residues conserved in VGLUTs alone are highlighted by red boxes. (**B**) Structure of the substrate binding site in VGLUT2. Glutamate was manually placed into the binding site to mimic D-galactonate in DgoT. Both R88 and R322 are located at distances suitable for interacting with the carboxyl groups. (**C**) Structure of the substrate binding site in DgoT with substrate D-galactonate bound in the outward occluded conformation [PDB: 6E9O (22)]. Structures of VGLUT2 (B) and DgoT (C) are colored following the same pattern as (A), and substrates are colored cyan. (**D**) mEPSCs recorded from hippocampal neurons of VGLUT1 and VGLUT2 double knockout (DKO) mice rescued with WT, R88A, and R322A VGLUT2. Synaptic transmission is impaired by the R88A mutation and eliminated by the R322A mutation. mEPSC frequency (left) and amplitude (right) are normalized to those of VGLUT2-WT ($n = 10$ to 15 cells per condition). Data indicate means and SEM. Statistical significance was determined by one-way analysis of variance (ANOVA) with Tukey's post hoc test. *$P < 0.05$; ***$P < 0.001$; ns, not significant. Single-letter abbreviations for the amino acid residues are as follows: A, Ala; C, Cys; D, Asp; E, Glu; F, Phe; G, Gly; H, His; I, Ile; K, Lys; L, Leu; M, Met; N, Asn; P, Pro; Q, Gln; R, Arg; S, Ser; T, Thr; V, Val; W, Trp; and Y, Tyr.

Author Manuscript Author Manuscript Author Manuscript Author Manuscript

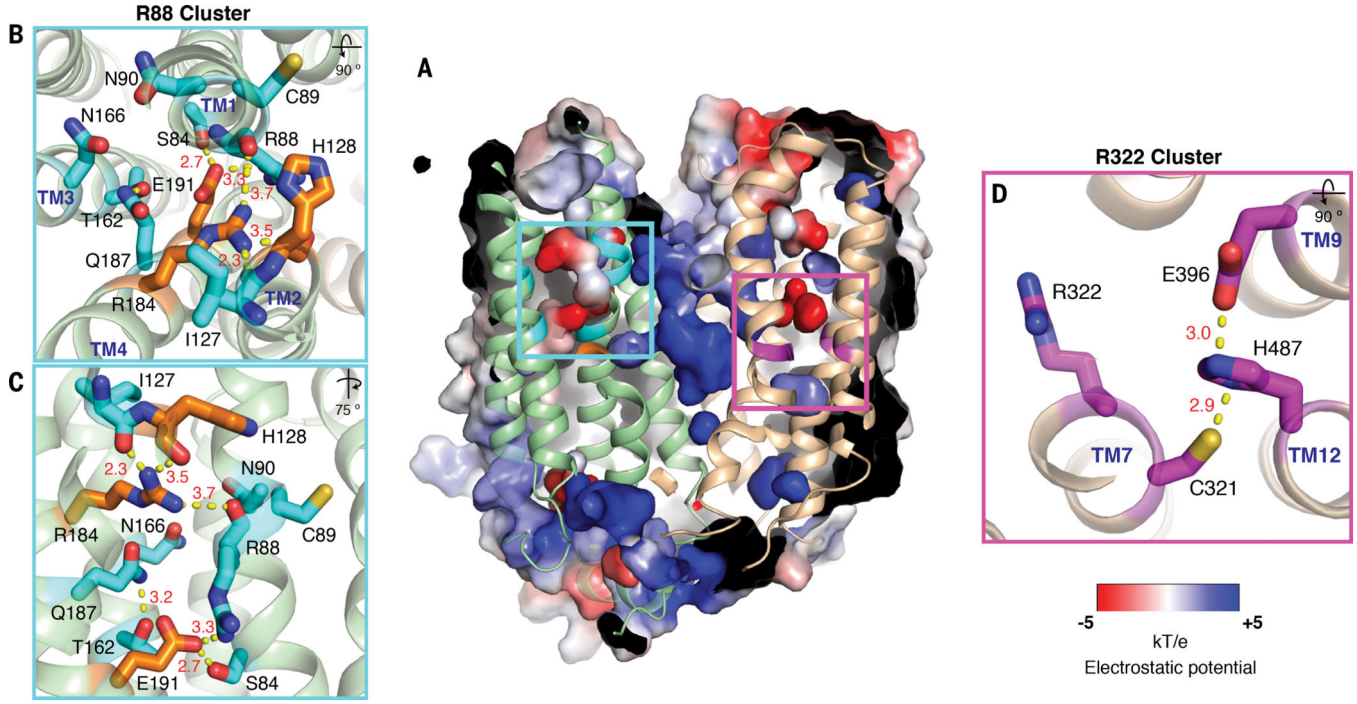

Fig. 3. Two functional clusters of charged and polar residues embedded within the transmembrane domains.

(**A**) Electrostatic surface of VGLUT2. Two internal charged and polar cavities (referred to as R88 and R322 clusters) are colored according to the potential scale (bottom right). The N-domain is colored light green and the C-domain is tan. Cyan and magenta boxes in (A) match the insets in (B) (top view), (C) (side view), and (D) (top view), showing key residues and distances between polar groups (A). (**B** and **C**) R88 cluster with proposed Cl^- (R184) and H^+ binding sites (E191 and H128) highlighted in orange. (**D**) R322 cluster.

Author Manuscript Author Manuscript Author Manuscript Author Manuscript

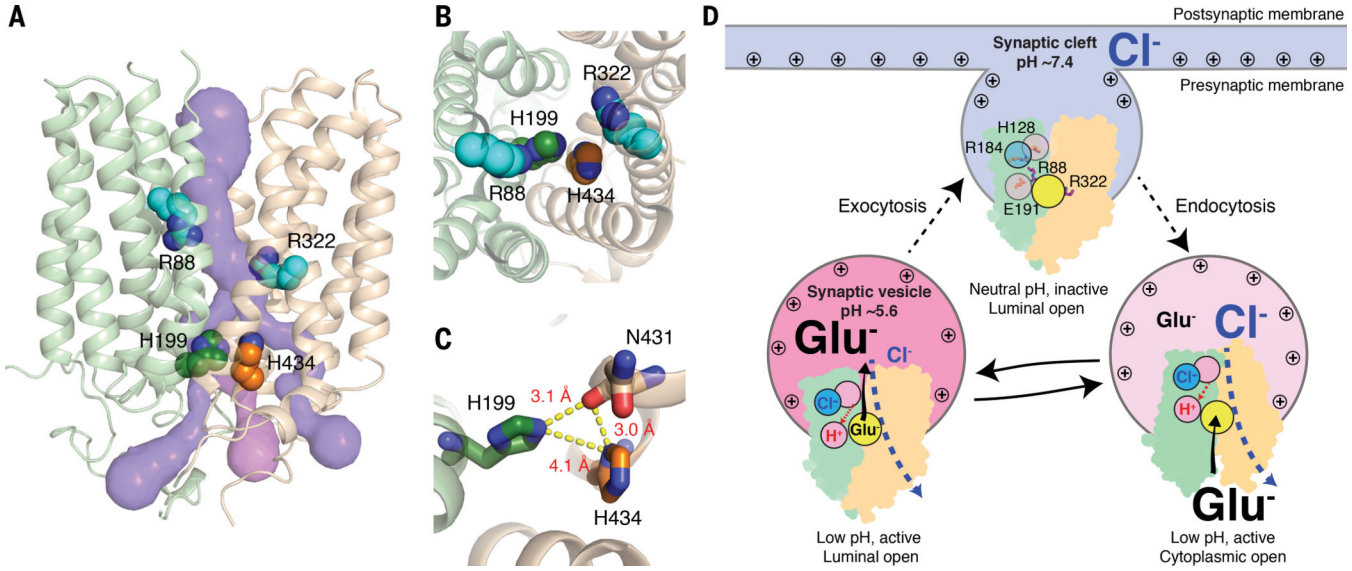

Fig. 4. Putative Cl^- channels and proposed transport mechanism.

(**A**) Channels consistent with Cl^- conductance (surface). (**B**) Top view of the central channel. (**C**) Top view of the cytoplasmic two-His gate. Distances (Å) between polar groups are shown with dotted lines. (**D**) Proposed mechanism by which VGLUT integrates the dynamic change of ionic conditions during synaptic vesicle recycling to regulate its activity.